Available online at www.sciencedirect.com
ScienceDirect
Journal of Nuclear Materials 363–365 (2007) 977–983
journal of nuclear materials
www.elsevier.com/locate/jnucmat

Dynamics of hydrogenic retention in molybdenum: First results from DIONISOS

G.M. Wright [a,*], D.G. Whyte [a], B. Lipschultz [b], R.P. Doerner [c], J.G. Kulpin [a]

[a] University of Wisconsin-Madison, 1500 Engineering Drive, Madison, WI 53706, USA
[b] M.I.T. Plasma Science and Fusion Center, 175 Albany Street, Cambridge, MA 02139, USA
[c] University of California-San Diego, 9500 Gilman Drive, La Jolla, CA 92093-0417, USA

Abstract

The DIONISOS (Dynamics of ION Implantation and Sputtering of Surfaces) experiment is described. DIONISOS features steady-state plasma exposure of material surfaces, with simultaneous, in situ, non-destructive depth profiling on the same surfaces with ion beam analysis (IBA). A steady-state RF helicon plasma source produces a fusion 'edge-like' low temperature ($T \sim 1$–10 eV), high-density ($\leqslant 10^{17-18}$ m^{-3}), steady-state, cylindrical, plasma ($\phi \sim 50$ mm). The exposure stage allows for the control of sample surface temperature (300–800 K), incident ion energy (10–500 eV), and ion beam and magnetic field incident angle (360° rotation), during bombardment with high plasma flux ($\sim 10^{20}$–10^{22} s^{-1} m^{-2}). First results from DIONISOS show a large and evolving concentration of deuterium ($\sim$1000 appm) trapped deep ($\sim$5 μm) in molybdenum. IBA during plasma exposures shows the surface dynamic deuterium inventory increased by a factor of 2 over the 'long-term' trapped inventory at an incident ion flux density of $\sim 1.5 \times 10^{21}$ D/m^2 s.

PACS: 25.55.−e; 28.52.Fa

Keywords: Molybdenum; Deuterium inventory; Retention; Surface analysis

1. Introduction

As experiments move towards longer discharges and to time scales at which thermal equilibrium can be obtained at the wall, a concern is how dynamic plasma–surface interactions will affect plasma operation, material lifetimes and tritium fuel retention. For example, a recent study of the fuel inventories and particle control during long-pulse discharges in JT-60U concluded that dynamic retention dominated the carbon wall fuel inventories [1]. The dynamic interplay between surfaces and the plasma should be expected in a fusion device given the high level of recycling and the sensitivity of the plasma behavior to impurities from wall erosion. For a long-pulse device that achieves quasi plasma–surface equilibrium, small changes in material properties (e.g. dynamic fuel retention rate) could strongly affect particle and performance control in a long-pulse discharge [2]. Unfortunately, the underlying cause of these dynamics must be inferred from plasma behavior, while the underlying

* Corresponding author. Fax: +1 608 265 2364.
E-mail address: gmwright@wisc.edu (G.M. Wright).

0022-3115/$ - see front matter © 2007 Elsevier B.V. All rights reserved.
doi:10.1016/j.jnucmat.2007.01.135

mechanism that controls the dynamics is actually the evolution of materials properties. Direct measurements of such material evolution are extremely difficult in a fusion device, due to the limitations of in situ plasma–surface interaction diagnostics. As more attention is focused on physics of long-pulse plasma discharges, such as for ITER, the demand to examine the dynamics of plasma–surface interactions increases.

The DIONISOS (Dynamics of ION Implantation and Sputtering Of Surfaces) experiment was designed to address these issues. The DIONISOS experiment probes the surface of a specimen using in situ ion beam analysis techniques while simultaneously exposing that same surface to a low temperature, high density, fusion 'edge-like' plasma. This allows for spatially and depth-resolved measurements of fuel inventory and material erosion/deposition, before, during, and after plasma exposure.

The focus of this article is two-fold: to describe the design and abilities of DIONISOS and to report its first results with regard to the dynamic and long-term retention of deuterium (D) fuel in molybdenum (Mo). High D retention rates seen recently in the Mo-clad Alcator C-Mod [3] substantially exceed retention rates measured in laboratory experiments [4–10]. These results, and the general interest in refractory metals for fusion (e.g. W in ITER), motivated these first experiments. Molybdenum specimens were taken from Alcator C-Mod and exposed at the PISCES-A experiment [11]. These specimens were analyzed with ex situ NRA, elastic recoil detection (ERD), and thermal desorption spectroscopy (TDS). The results from the PISCES-A exposures were used to scope exposure conditions for DIONISOS. Molybdenum plates and foils were exposed to a range of plasma fluence and flux densities in DIONISOS. Depth-resolved deuterium concentrations were made with in situ ^{3}He nuclear reaction analysis (NRA). The ability to directly measure dynamic retention allows us to infer underlying surface processes such as deuterium diffusion, trapping and surface recombination, which can eventually be applied to tokamak situations.

2. Experiment

2.1. The DIONISOS experiment

The DIONISOS experiment is designed to allow simultaneous plasma exposure and ion beam analysis (IBA) of a sample surface. To achieve this, a helicon plasma exposure chamber was mounted on the end of a 1.7 MeV tandem ion accelerator beam line (see Fig. 1). DIONISOS is comprised of three main components: the exposure chamber (vacuum vessel, sample holder, cooling system, etc.), the helicon plasma source, and the ion accelerator used as the main diagnostic for the experiment.

The DIONISOS facility is designed to provide abundant diagnostic and physical access to the specimen surface and to recreate a large range of surface conditions for plasma exposures. The DIONISOS vacuum vessel is a custom-built chamber with 19 diagnostic ports, 5 of those being line-of-sight ports onto the sample surface. A hinged door on the back of the vessel allows for easy access to the interior of the chamber and the sample holder. This allows for quick change of samples although vacuum must be broken to do so. Vacuum of $\sim 10^{-6}$ Pa has been achieved, although typical vacuum tends to be closer to $\sim 10^{-5}$ Pa.

The DIONISOS sample holder can recreate a large range of surface conditions while maintaining flexible attachment for a large variety of sample shapes and sizes. Samples are mounted to a 10 cm × 9 cm copper plate heat sink suspended in the vessel from above. The only shape requirement is that good mechanical and thermal contact to the flat copper heat sink can be obtained. The sample holder is mounted on a 360° rotatable platform, which allows for a full control over the incident angle of the ion beam or axial magnetic field (although the angle between the field and ion beam is fixed at 45°). The heat sink has both water and air cooling capabilities and active heating for temperature control ranging from 300 to 800 K using a feedback control with thermocouples and resistive temperature devices (RTD). Surface temperature can also be monitored with infrared imaging. The sample holder is electrically floating with respect to the chamber walls, which allows the sample to be actively biased up to 600 V, thus controlling incident ion energy. The entire heat sink can be removed for maintenance or to be replaced with another custom heat sink for samples of inconvenient shape (rods, spheres, etc.).

The DIONISOS plasma source is an RF helicon plasma supply. The helicon mode provides high density and low temperature plasmas for an RF source. The source consists of an $m = 1$ Nagoya type III antenna surrounding a cylindrical quartz tube. The antenna is attached to a 5 kW RF power supply through a manual match network. Typical

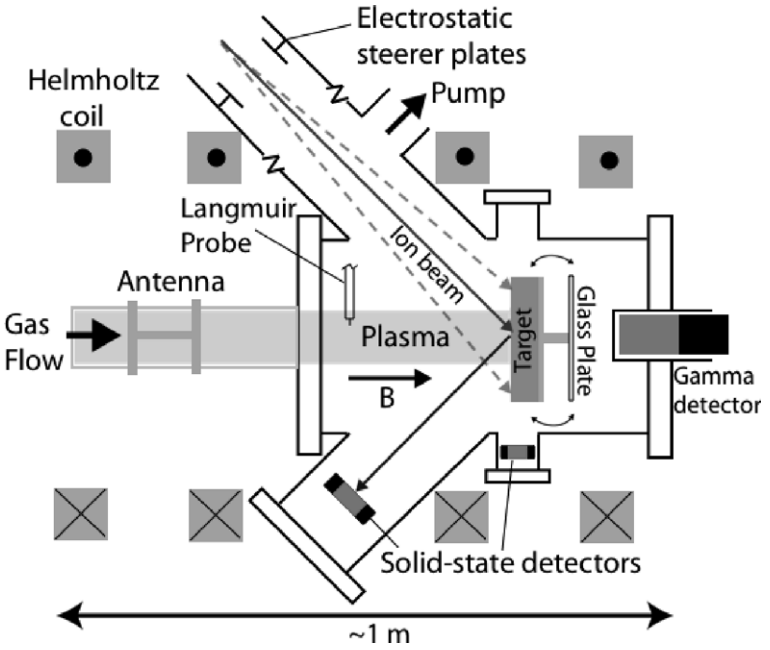

Fig. 1. A schematic of the DIONISOS experiment.

helicon plasmas have <5% reflected power. Plasma parameters are measured by a scanning Langmuir probe in the exposure chamber ~10 cm from the target. Deuterium plasma flux density and electron temperature have been measured across the plasma column (e.g. Fig. 2). The plasma flux density follows a Gaussian curve peaked at the center of the column. This Gaussian shape has been confirmed by IR thermography of the plasma footprint. The Gaussian shape of the flux density provides the ability to measure the effects of various plasma flux densities by simply re-steering the ion beam to analyze different radial locations within the column. The electron temperature profile is fairly flat across the plasma column ranging from 4 to 6 eV. The quartz tube and DIONISOS chamber are surrounded by a set of four Helmholtz coils with a maximum axial magnetic field of ~1 kG. The plasma is confined by the magnetic field and extracted from the source resulting in a cylindrical plasma on target. Neutral gas is fed into the back of the quartz tube and gas flow is controlled by a mass flow controller. Neutral gas pressure inside the vacuum vessel is measured by a capacitance manometer during plasma operations. Typical neutral pressures for deuterium plasmas are ~0.3–1 Pa.

A 1.7 MV Pelletron tandem ion accelerator is used to produce ion beams for IBA of sample surfaces. The ion accelerator provides ions with energies of ⩽10 MeV. An energy feedback loop keeps the beam monoenergetic to within ~1 keV. Ion

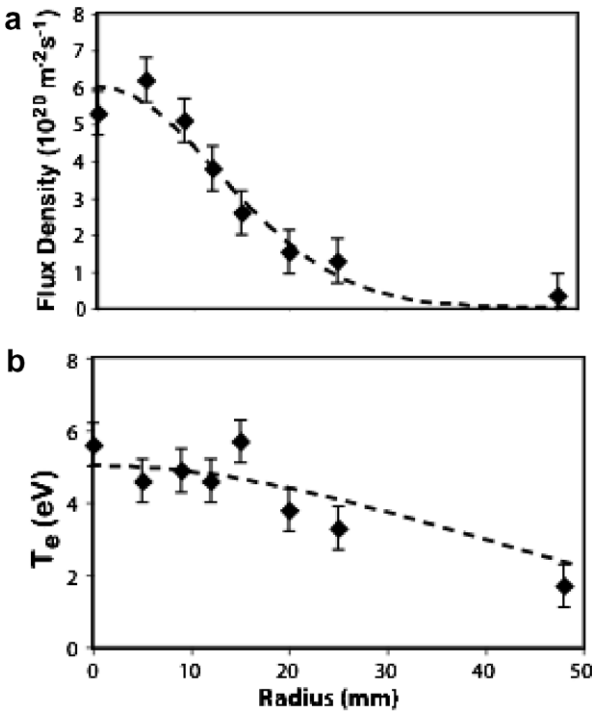

Fig. 2. The (a) ion flux density and (b) electron temperature as a function of plasma radius. Measurements were taken ~10 cm from the target plate for a deuterium plasma with $B = 500$ G, $P_{RF} = 500$ W, and $p_D = 0.8$ Pa.

beam currents of 100's μA can be achieved, but typical beam currents for surface analysis are 0.5–3 μA to ensure that they are not perturbing the surface. The beam spot can be magnetically focused on the target to a spot diameter of ~2 mm. Magnets and electrostatic steerer plates are also used to move the beam spot both horizontally and vertically across a sample surface. DIONISOS has no limiting apertures so that all locations on the target are accessible to the ion beam. Horizontal and vertical control of a very tight beam spot allows for detailed spatial scans of material surfaces, e.g. radial erosion/deposition profiles as might be found near a divertor strikepoint.

Most standard IBA techniques are available on DIONISOS: nuclear reaction analysis (NRA), particle-induced gamma emission (PIGE), elastic recoil detection (ERD), and Rutherford backscattering (RBS). Solid-state charged particle detectors are used to detect reaction products or scattered particles. The data acquired by the solid-state detectors is fit using the SIMNRA simulation [12], yielding a non-destructive depth-resolved layer structure of the elemental composition of the surface. The ion beam is checked to be non-perturbing since repeated IBA on the same spot yield the same spectra.

During simultaneous IBA and plasma exposure of a surface, the large energy gap between beam ions and plasma ions allows these ions to act independently of one another. The stopping distance for a beam ion in the exposure chamber plasma ($n_{gas} < 10^{20}\ m^{-3}$) is $>10^3$ m, so there is little to no interaction. However, atoms sputtered off the sample surface with $E \sim$ eV will have a mean free path of ~cm, i.e. the sputtered particle can be ionized and re-deposited before escaping the plasma column, similar to recycling in a tokamak. The axial magnetic field used for the helicon plasma source can deflect the incident ion beam. However, since the beam can be visually aligned with the field on, any deflection (typically $\leqslant$1 cm for most ion beam and magnetic field combinations) can be compensated for with electrostatic steering plates.

2.2. Molybdenum samples

Two types of Mo samples were exposed in DIONISOS, a polycrystalline 10 cm × 10 cm × 1.6 mm 99.97% Mo plate from Ed Fagan Inc. and a polycrystalline 10 cm × 10 cm × 25 μm 99.99% Mo foil from Elmet Technologies. Both samples were cleaned with alcohol before exposure but no other sample preparation was performed on either sample.

The plasma exposure conditions for the Mo plate were $E_D = 100$ eV, $T_e \sim 5$ eV with a peak ion flux density of $\sigma_D = 1.8 \times 10^{21}\ D/m^2\ s$. The Mo plate was actively water cooled during plasma exposure and the sample temperature was measured to be $\leqslant$310 K. For the Mo foil, plasma parameters were $E_D = 100$ eV, $T_e \sim 5$ eV with a peak ion flux density of $\sigma_D = 8 \times 10^{20}\ D/m^2\ s$. The Mo foil was actively water cooled, but due to poorer thermal contact with the heat sink, the surface was heated to ~400 K by the plasma. Once the plasma was removed, the surface temperature returned to ~300 K in <10 s.

An incident ion beam of 3.5 MeV $^3He^{++}$ was used to detect deuterium up to ~5 μm into the surface using the $^3He(d,p)^4He$ nuclear reaction.

3. Results and discussion

3.1. 25 μm Mo foil at 370 K

A fluence scan was performed on the Mo foil at 400 K (see Fig. 3) at the center of the plasma column. The deuterium concentrations were obtained in situ ~100 s after plasma exposure, but with no plasma present on the sample. After a fluence of $2.5 \times 10^{23}\ D/m^2$, the deuterium already appears at depths >1 μm, and at high concentrations (~3500 appm) near the surface. As the fluence increases, the deuterium moves deeper into the sample until at a fluence of $1.7 \times 10^{24}\ D/m^2$ the deuterium extends past the maximum detection depth, ~5 μm, of the 3.5 MeV ^3He ions. The deuterium concentration at all depths increases with incident fluence showing no signs of

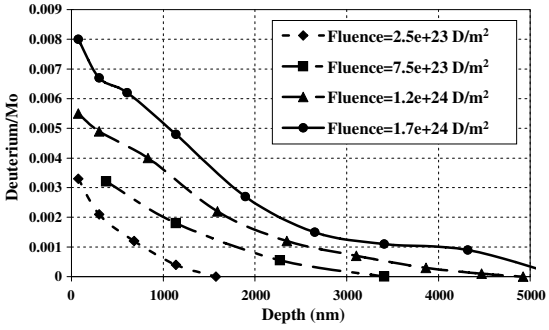

Fig. 3. Depth profiles of the trapped D concentration in the 25 μm Mo foil for four different ion fluences (taken after plasma exposure). These measurements were performed at the center of the plasma-exposed area.

local saturation. At the maximum fluence of 1.7×10^{24} D/m^2, the concentration of deuterium at the surface is ~8000 appm.

At an ion energy of 100 eV/D$^+$, there are no vacancies produced in the Mo by the deuterium (nor sputtering of Mo). However, evolving trapped deuterium concentrations up to ~8000 appm indicate trap production in the surface region. The mechanism of this inferred trap production is unknown and requires further study. One possibility is pressure-induced trap production due to the high flux of implantation at low energies, similar to void or blister formation [13,14]. Depth profiles of 10 keV D$^+$ implanted in Mo were measured by Nagata et al. [7]. For a fluence of $\sim 1 \times 10^{22}$ D/m^2 at 346 K, the deuterium was detected at depths up to 4 μm but the concentration in the first micron of the surface was reduced as compared to a 298 K exposure. In the exposures on DIONISOS, the concentration at the surface continues to rise as the trapped deuterium appears to diffuse into the bulk. This discrepancy may be due to the higher flux densities achieved in DIONISOS ($\sim 1 \times 10^{21}$ D/m^2 s) than by Nagata et al. ($\sim 1 \times 10^{18}$ D/m^2 s), allowing for a greater fraction of surface traps to be occupied before the implanted D can diffuse into the bulk. The high ion energies (10 keV/D) used by Nagata et al. as opposed to the much lower DIONISOS ion energies (100 eV/D) may also be playing a role in terms of trap production.

Since the deuterium is detected much deeper than the implantation range of 100 eV D$^+$ in Mo (~2 nm), it is clear that the trapped deuterium is migrating further away from the implantation zone. The total plasma fluence was obtained over an exposure time of ~2100 s. Taking measured deuterium diffusion rates in Mo [15–18] and extrapolating the fits to $T = 400$ K, the diffusion length scales associated with a time scale of 2100 s range from 3.5 to 1400 μm. Because of the large scatter of measured deuterium diffusion rates in Mo, it is unclear if the diffusion that is occurring in the Mo foil is deuterium diffusing through Mo or *trap sites* diffusing from the surface into the bulk of the sample. Whatever the cause, it is clear that the plasma exposure itself is evolving the trapped deuterium profiles in the Mo.

3.2. 1.6 mm thick Mo plate at 300 K

Both the dynamic (with plasma on) and trapped (plasma off) inventories were measured for the Mo plate in DIONISOS (Fig. 4). The Mo plate was previously exposed to deuterium plasmas, which is why the initial retained fluence is not zero. The inventories were determined by integrating the measured deuterium concentration profile over the entire detection depth.

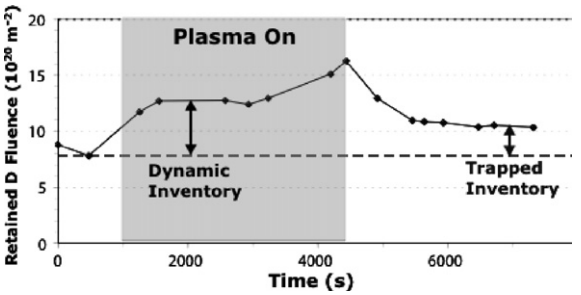

Fig. 4. NRA measured retained D fluence in the Mo plate in real-time; before, during, and after a deuterium plasma exposure with flux density of 1.8×10^{21} D/m^2 s and $V_{bias} = 100$ V.

It is clear that the presence of the plasma has an immediate effect on the deuterium inventory. In the presence of the plasma, the deuterium inventory increases by ~50% but continues to evolve and increase with passing time. NRA shows that the dynamically stored D is in the first 500 nm of the surface By the end of the exposure, the dynamic inventory is a factor of 2–3 greater than the pre-exposure inventory. This continuing evolution of the dynamic inventory may be another indication of trap production in the implantation zone by low-energy, high flux plasmas.

Once the plasma is removed, the Mo plate no longer has a source of ions into its surface. The deuterium inventory evolves as the implanted, but non-trapped, deuterium is released from the surface. The deuterium inventory decays to a steady-state inventory that is representative of trapped deuterium. The asymptotic trapped deuterium inventory is ~25% greater than the pre-exposure inventory, indicating long-term trapping.

The dynamic inventory enhancement is a factor of 2 greater than the increase in the trapped inventory. Previous dynamic inventory measurements made on carbon by Emmoth et al. [19] also show an enhanced dynamic inventory in carbon. Initial results on Mo indicate that the dynamic inventory increases as the square-root of incident flux density (obtained by NRA on different radial locations). The square-root dependence is consistent with the surface recombination limiting the deuterium release as molecules assuming the recombination

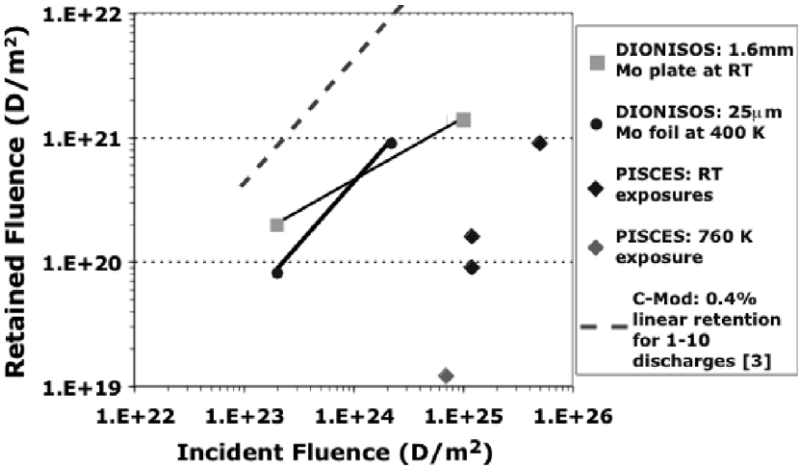

Fig. 5. A comparison of D retention results obtained on the DIONISOS experiment with results from wall-pumping experiments on Alcator C-Mod [3] and ex situ analysis of Mo exposed at PISCES-A. The PISCES-A samples were thermally desorbed at 1300 K before exposure.

sites are not saturated [20]. The post-exposure inventory decreases with ~500 s e-folding time. The deuterium inventory reaches equilibrium, showing that the ion beam is non-perturbing in this case.

Overall retention rates (scaled to incident ion fluence) from the DIONISOS experiment (to-date) are compared to the observed retention rates in Alcator C-Mod results from ex situ analysis of Mo exposed in PISCES-A (see Fig. 5). As with C-Mod, no sign of D retention saturation is found. The retention magnitude from DIONISOS is larger than seen with ex situ analysis. The PISCES-A samples were thermally desorbed at 1300 K for ~600 s before plasma exposure. This thermal desorption may have an annealing effect on the sample and reduce the retention rates in subsequent exposures [21]. The DIONISOS results are ~5–10 times smaller than found for C-Mod. This requires further study.

4. Conclusions

Deuterium implanted into Mo with a low energy, high flux plasma can be found at depths in excess of 5 μm. The maximum deuterium concentration found in the surface region was ~8000 appm although there were no indications that this was a saturation level, so concentrations may continue to increase with increasing fluence. There is also strong evidence of trap production in the surface region by exposure to a low-E, high flux plasma. No mechanism has been confirmed for this trap production. Overall retention linearly increases with fluence at 400 K, ~0.05% retained per incident ion, although this is still smaller than inferred from C-Mod experiments.

Measurements of the dynamic inventory of deuterium in Mo show that the dynamic inventory is enhanced over the trapped inventory by a factor of 2–3. Early results also indicate the dynamic inventory scales as the square-root of incident flux, consistent with surface recombination limiting D molecular release.

Acknowledgements

This work was supported by US Department of Energy Plasma Physics Junior Faculty Development award, DE-FG02-03ER54727. Our thanks are extended to Christopher Chrobak, Joshua Shea, and Soren Harrison for their assistance in the design and construction of the DIONISOS experiment.

References

[1] T. Nakano, N. Asakura, H. Takenaga, H. Kube, Y. Miura, K. Shimzu, S. Konoshima, K. Masaki, S. Higashijima, The JT-60 Team, Nucl. Fusion 46 (2006) 626.
[2] S.I. Krasheninnikov, T.K. Soboleva, Phys. Plasmas 13 (2006) 094502.
[3] B. Lipschultz, Y. Lin, M.L. Reinke, D. Whyte, A. Hubbard, I.H. Hutchinson, J. Irby, B. LaBombard, E.S. Marmar, K. Marr, J.L. Terry, S.M. Wolfe, the Alcator C-Mod group, J. Nucl. Mater., these Proceedings, doi:10.1016/j.jnucmat.2007.01.227.
[4] R.A. Causey, C.L. Kunz, D.F. Cowgill, J. Nucl. Mater. 337–339 (2005) 600.
[5] S. Nagata, K. Takahiro, S. Horiike, S. Yamaguchi, J. Nucl. Mater. 266–269 (1999) 1151.

[6] K. Yamaguchi, M. Okada, O. Onoue, F. Ono, M. Yamawaki, J. Nucl. Mater. 258–263 (1998) 1104.
[7] S. Nagata, T. Hasunuma, K. Takahiro, S. Yamaguchi, J. Nucl. Mater. 248 (1997) 9.
[8] A.A. Haasz, J.W. Davis, J. Nucl. Mater. 241–243 (1997) 1076.
[9] R. Sakamoto, T. Muroga, N. Yoshida, J. Nucl. Mater. 233–237 (1996) 776.
[10] K.L. Wilson, R. Bastasz, R.A. Causey, D.K. Brice, B.L. Doyle, W.R. Wampler, W. Möller, B.M.U. Scherzer, T. Tanabe, Nucl. Fusion Suppl. (1991) 31.
[11] D.M. Goebel, Y. Hirooka, R.W. Conn, W.K. Leung, G.A. Campbell, J. Bohdansky, K.L. Wilson, W. Bauer, R.A. Causey, A.E. Pontau, A.R. Krauss, D.M. Gruen, M.H. Mendelson, J. Nucl. Mater. 145–147 (1987) 61.
[12] M. Mayer, In: American Institute of Physics Conference Proceedings 475 (1999) 571.
[13] A.A. Haasz, M. Poon, J.W. Davis, J. Nucl. Mater. 266–269 (1999) 520.
[14] J.B. Condon, T. Schober, J. Nucl. Mater. 207 (1993) 1.
[15] T. Tanabe, Y. Furuyama, S. Imoto, J. Nucl. Mater. 191–194 (1992) 439.
[16] H. Katsuta, R.B. McLellan, K. Furukawa, J. Phys. Chem. Solids 43 (1982) 533.
[17] G.R. Caskey Jr., M.R. Louthan, R.G. Derrick, J. Nucl. Mater. 55 (1975) 279.
[18] T. Tanabe, Y. Furuyama, N. Saitoh, S. Imoto, Trans. Jap. Inst. Metals 28 (1987) 706.
[19] B. Emmoth, H. Bergsaker, L. Ilyinsky, J. Nucl. Mater. 241–243 (1997) 1022.
[20] W.R. Wampler, J. Appl. Phys. 69 (1991) 3063.
[21] T. Venhaus, J. Nucl. Mater. 290–293 (2001) 505.